Yuan *et al.*
Chinese Journal of Mechanical Engineering (2022) 35:121
https://doi.org/10.1186/s10033-022-00794-1

Chinese Journal of Mechanical Engineering

ORIGINAL ARTICLE

Open Access

Theoretical Model of Dynamic Bulk Modulus for Aerated Hydraulic Fluid

Xiaoming Yuan[1,2,3*], Weiqi Wang[1,2], Xuan Zhu[1,2] and Lijie Zhang[1,2]

Abstract

Existing models of bulk modulus for aerated hydraulic fluids primarily focus on the effects of pressure and air fraction, whereas the effect of temperature on bulk modulus is disregarded. Based on the lumped parameter method and the full cavitation model, combined with the improved Henry's law and the air polytropic course equation, a theoretical model of dynamic bulk modulus for an aerated hydraulic fluid is derived. The effects of system pressure, air fraction, and temperature on bulk modulus are investigated using the controlled variable method. The results show that the dynamic bulk modulus of the aerated hydraulic fluid is inconsistent during the compression process. At the same pressure point, the dynamic bulk modulus during expansion is higher than that during compression. Under the same initial air faction and pressure changing period, a higher temperature results in a lower dynamic bulk modulus. When the pressure is lower, the dynamic bulk modulus of each temperature point is more similar to each other. By comparing the theoretical results with the actual dynamic bulk modulus of the Shell Tellus S ISO32 standard air-containing oil, the goodness-of-fit between the theoretical model and experimental value at three temperatures is 0.9726, 0.9732, and 0.9675, which validates the theoretical model. In this study, a calculation model of dynamic bulk modulus that considers temperature factors is proposed. It predicts the dynamic bulk modulus of aerated hydraulic fluids at different temperatures and provides a theoretical basis for improving the analytical model of bulk modulus.

Keywords: Aerated hydraulic fluid, Dynamic bulk modulus, Theory model, Air fraction, Pressure

1 Introduction

Hydraulic fluid power systems offer a large power-to-weight ratio, good stationarity, and high reliability. Owing to these advantages, hydraulic fluid power systems have been widely used in the engineering community [1–4]. In a hydraulic system, the operating medium containing a minute amount of free air is referred to as an aerated hydraulic fluid. Many factors affect the accuracy and energy efficiency of a hydraulic system, including system control strategies, structural forms, and external incentives [5–8]. In addition, the properties of aerated hydraulic fluids significantly affect the performance of hydraulic systems. The bulk modulus, which is an important parameter for characterizing the compressing characteristics of aerated hydraulic fluids, affects the efficiency and operational stability of hydraulic transmission systems [9–12]. The bulk modulus of an aerated hydraulic fluid is affected by many factors, such as fluid pressure, air fraction of the aerated hydraulic fluid, and temperature [13, 14]. Owing to the operating conditions, the fluid of the system inevitably undergoes dissolution, cavitation, and vaporization as a result of the acute change in pressure. Therefore, the air fraction of the fluid changes frequently, resulting in dynamic changes in the bulk modulus of the aerated hydraulic fluid [15, 16]. In studies pertaining to the bulk modulus of aerated hydraulic fluids, some scholars established theoretical models (steady-state models) based on their belief that the air fraction of the fluid is associated with only pressure [17]. Others believe that both the relationship between the air fraction of the fluid and pressure change, and the time

*Correspondence: xiaomingbingbing@163.com

[1] Hebei Key Laboratory of Heavy Machinery Fluid Power Transmission and Control, Yanshan University, Qinhuangdao 066004, China
Full list of author information is available at the end of the article

effect of various factors (dynamic model) must be considered [18–20].

Steady-state models do not consider the non-equilibrium state of air components during transportation, i.e., the dynamic process of air release and dissolution is disregarded. Consequently, they cannot accurately describe the dynamic change process of the bulk modulus. Meanwhile, dynamic models consider the time effect of air components in aerated hydraulic fluids with pressure change; as such, the release and dissolution of air in the model is a dynamic process that changes with pressure and time [21].

Singhal et al. [22] derived a formula for the phase transition rate of aerated hydraulic fluids in the cavitation course by applying the Rayleigh–Plesset equation to describe bubble dynamics and established a full cavitation model. Zhou et al. [23] performed experiments using the full cavitation model as a basic model. Subsequently, they proposed a dynamic equation for the oil vapor fraction, established a dynamic cavitation model of for a two-phase system comprising oil and air, and validated the theory of bulk modulus for aerated hydraulic fluids. Sakama et al. [24] experimentally demonstrated that the dynamic differences between the dissolution and release course of air significantly affected the bulk modulus of an aerated hydraulic fluid.

The steady-state model of bulk modulus mentioned above satisfies practical engineering demands within a certain range; however, for transmission conditions under high speeds and pressures, the dynamic model can describe the real-time characteristics of the transmission system more accurately. However, because the dynamic model does not consider the effect of temperature variation on the bulk modulus during calculation, the accuracy of the dynamic model must be further improved. In fact, in a dynamic hydraulic transmission system at high speeds and pressures, the temperature of the aerated hydraulic fluid inevitably changes owing to frequent system movements [25, 26]. Kim and Bin Feng et al. experimentally measured the bulk modulus of a hydraulic oil at various temperatures, and their results indicated that temperature variation significantly affected the bulk modulus [27, 28]. Therefore, in the dynamic model of bulk modulus, the effect of temperature variation should be considered to reflect the dynamic characteristics of hydraulic systems more accurately.

Currently, most dynamic models for aerated hydraulic fluids primarily consider the effects of pressure and air fraction of fluid on the bulk modulus. Although the bulk modulus of aerated hydraulic fluids at different temperatures have been measured experimentally, theoretical calculation formulas have not been derived. Therefore, a dynamic model of an aerated hydraulic fluid is introduced herein. In the dynamic model, the lumped parameter method is adopted, thermodynamic parameters are introduced by considering the full cavitation model as a basic model, and the change law of the air component state in the fluid when the temperature changes is analyzed. Subsequently, the effects of the initial air fraction, pressure changing cycle, and temperature variation on the dynamic bulk modulus were evaluated by calculating the dynamic bulk modulus of the Shell Tellus S ISO32 standard air-containing oil. The precision of the derived theoretical model was verified by comparing the theoretical results with the experimental data. The aim of this study is to provide evidence for the theory and actual application of the dynamic bulk modulus of aerated hydraulic fluids.

2 Theory Model

2.1 Dynamic Mass Fraction of Air Components

2.1.1 Dynamic Mass Fraction of Vapor

Singhal et al. [22] proposed a transmission equation for computing the vapor mass fraction while computing the dynamic fraction of vapor in an aerated hydraulic fluid.

$$\frac{\partial}{\partial t}\left(\rho f_{\mathrm{v}}\right)+\nabla\cdot\left(\rho\mathbf{U}f_{\mathrm{v}}\right)=\nabla\cdot\left(\Gamma\nabla f_{\mathrm{v}}\right)+R, \tag{1}$$

where t represents time (s), $\mathbf{U}$ the transmission rate of vapor, ρ the density of the aerated hydraulic fluid (kg/m^3), f_{v} the vapor mass fraction of the aerated hydraulic fluid, and R the phase change speed between liquid and vapor.

We assume that fluid attributes, such as the density and pressure of the fluid in the control volume, are uniformly distributed. Therefore, Eq. (1) can be simplified to the following form by disregarding the diffusive term, where the position derivative is used as the basis in the transmission equation:

$$f_{\mathrm{v}}\frac{\mathrm{d}\rho}{\mathrm{d}t}+\rho\frac{\mathrm{d}f_{\mathrm{v}}}{\mathrm{d}t}=R, \tag{2}$$

Typically, the density of an aerated hydraulic fluid typically does not change significantly when cavitation occurs and $\frac{\mathrm{d}\rho}{\mathrm{d}t}<<\frac{\mathrm{d}f_{\mathrm{v}}}{\mathrm{d}t}$. Thus, Eq. (1) can be further simplified as follows:

$$\frac{\mathrm{d}f_{\mathrm{v}}}{\mathrm{d}t}=R_{\mathrm{s}}, \tag{3}$$

where R_{s} is the simplified phase change speed.

From the perspective of bubble collapse and formation in liquid, the bubble dynamics equation derived from the Rayleigh–Plesset equation can be used to calculate the phase transition rate between the liquid and vapor, as follows:

$$R_{\mathrm{B}}\frac{\mathrm{d}^2R_{\mathrm{B}}}{\mathrm{d}t^2}+\frac{3}{2}\left(\frac{\mathrm{d}R_{\mathrm{B}}}{\mathrm{d}t}\right)^2=P-\frac{4\nu_{\mathrm{l}}}{R_B}\frac{\mathrm{d}R_{\mathrm{B}}}{\mathrm{d}t}-\frac{2\sigma}{\rho_{\mathrm{l}}R_{\mathrm{B}}},\quad(4)$$

where R_{B} is the bubble radius (m), ν_{l} the fluid kinematic viscosity (m^2/s), σ the surface tension coefficient of the liquid (N/m), P the ratio of the difference between the internal pressure of the bubble and the pressure of the fluid to the density of the liquid, and ρ_{l} the density of the liquid ($\mathrm{kg/m}^3$).

P is expressed as

$$P=\left(\frac{p_{\mathrm{B}}-p}{\rho_{\mathrm{l}}}\right),\quad(5)$$

where p_{B} is the internal pressure of the bubble (Pa), and p is the pressure of the fluid (Pa).

The surface tension coefficient σ is computed as follows [29, 30]:

$$\sigma=\sigma_0\left(1-\frac{T}{T_{\mathrm{c}}}\right)^{\delta},\quad(6)$$

where σ_0 is initial surface tension coefficient of the liquid (N/m), T_{c} the critical temperature of the liquid (K), T the system operating temperature (K), and δ a global exponent.

Based on the derivation process of the full cavitation model and the bubble dynamics equation, as well as disregarding the viscosity term in the equation, the net phase transition rate can be expressed as [15]

$$R=\frac{3\alpha_{\mathrm{v}}}{R_{\mathrm{B}}}\frac{\rho_{\mathrm{v}}\rho_{\mathrm{l}}}{\rho^2}\left[\frac{2}{3}P-\frac{2}{3}\frac{2\sigma}{\rho_{\mathrm{l}}R_{\mathrm{B}}}-\frac{2}{3}R_{\mathrm{B}}\frac{\mathrm{d}^2R_{\mathrm{B}}}{\mathrm{d}t^2}\right]^{1/2},\quad(7)$$

where α_{v} is the volumetric vapor fraction of the aerated hydraulic fluid, and ρ_{v} is the density of the vapor ($\mathrm{kg/m}^3$).

By substituting R into Eq. (7) and disregarding the second-order derivative of the bubble radius, the following formula is obtained:

$$\frac{\mathrm{d}f_{\mathrm{v}}}{\mathrm{d}t}=\frac{3\alpha_{\mathrm{v}}}{R_{\mathrm{B}}}\frac{\rho_{\mathrm{v}}\rho_{\mathrm{l}}}{\rho^2}\left[\frac{2}{3}P-\frac{2}{3}\frac{2\sigma}{\rho_{\mathrm{l}}R_{\mathrm{B}}}\right]^{1/2},\quad(8)$$

where α_{v} can be expressed as a function of f_{v} as follows:

$$\alpha_{\mathrm{v}}=f_{\mathrm{v}}(t)\frac{\rho}{\rho_{\mathrm{v}}},\quad(9)$$

By assuming that all bubbles have the same radius and that the balance between aerodynamic drag and liquid surface tension determines the bubble radius, R_{B} can be calculated as follows [30]:

$$R_{\mathrm{B}}=\frac{0.061W\sigma}{2\rho_{\mathrm{l}}\nu_{\mathrm{rel}}^2},\quad(10)$$

where W is the Weber number.

For an aerated hydraulic fluid containing bubbles, ν_{rel} is the relative velocity of the aerated hydraulic fluid, whose value is relatively small, i.e., 5%–10% of the mean velocity of the fluid. By substituting Eqs. (9) and (10) into Eq. (8), the following equation is obtained:

$$\frac{\mathrm{d}f_{\mathrm{v}}}{\mathrm{d}t}=\frac{6\nu_{\mathrm{rel}}^2}{0.061W\sigma}\frac{\rho_{\mathrm{l}}\rho_{\mathrm{l}}}{\rho}\left|P'-\frac{2}{3}\frac{4\nu_{\mathrm{rel}}^2}{0.061W}\right|^{1/2}f_{\mathrm{v}},\quad(11)$$

Here,

$$P'=\frac{2}{3}\frac{p_{\mathrm{v}}-p}{\rho_{\mathrm{l}}},\quad(12)$$

where p_{v} is the saturated vapor pressure (Pa).

Using the analysis methods presented in Refs. [22, 23], ν_{rel}^2 can be expressed as a function of two components: one is $\sqrt{k}$, which is the delegate of the flowing state of the fluid; and the other is a component simplified with the parameters in Eq. (11), such as the Weber number and the surface tension coefficient to the vapor condensation coefficient a_{11} for characterizing the speed of vapor condensation. Thus, when the pressure of the aerated hydraulic fluid remains higher than the saturation vapor pressure, the coagulation of vapor can be described as

$$\frac{\mathrm{d}f_{\mathrm{v}}}{\mathrm{d}t}=a_{11}\sqrt{k}\frac{\rho_{\mathrm{l}}\rho_{\mathrm{l}}}{\rho}\left[\left|P'-\frac{4}{9}a_{11}\sigma\sqrt{k}\right|\right]^{1/2}f_{\mathrm{v}}.\quad(13)$$

Subsequently, the formula for turbulent energy can be used to calculate the turbulent energy of the aerated hydraulic fluid, as follows:

$$k=\frac{3}{2}(\mu l)^2,\quad(14)$$

where μ is the mean velocity (m/s), and l is the turbulence intensity.

The condensation of vapor is associated with the vapor mass fraction, and during vaporization, residual liquid is regarded as the source of vapor. Therefore, analogous to Eq. (13) is a polynomial function of pressure. The segmented expression for the air mass fraction is

$$\frac{\mathrm{d}f_{\mathrm{v}}}{\mathrm{d}t}=a_{12}\sqrt{k}\frac{\rho_{\mathrm{v}}\rho_{\mathrm{l}}}{\rho}\left[\left|P'-\frac{4}{9}a_{12}\sigma\sqrt{k}\right|\right]^{1/2}\left(1-f_{\mathrm{v}}-f_{\mathrm{g0}}\right),\quad(15)$$

where a_{12} is the vaporization coefficient of the vapor, and f_{g0} is the initial air mass fraction in the aerated hydraulic fluid.

2.1.2 Dynamic Mass Fraction of Air

The air pressure required to release air in an aerated hydraulic fluid is typically higher than the saturated vapor pressure required for vaporization. Cavitation typically involves a significant amount of air released from an aerated hydraulic fluid in a short duration and a rapid collapse of gas or vapor bubbles when the pressure increases. Because air constitutes the air phase in an aerated hydraulic fluid, the Rayleigh–Plesset equation can be applied to describe the release and dissolution of air. In addition to Eqs. (11) and (15), the following assumptions can be applied as bases for obtaining the air release and dissolution equation:

1. f_{gH} is the theoretical target value of the air mass fraction (steady-state value) when the pressure function time is sufficiently long. Meanwhile, when the transient pressure remains below the saturation vapor pressure, all of the dissolved air should be released. When the transient pressure remains above the air apart pressure, all free air should dissolve, which results in a f_{gH} of zero. Subsequently, using the improved Henry's law, when the transient pressure is within the ranges of the saturation vapor and air apart pressures, the target value of f_{gH} is a polynomial function of pressure. The segmented expression of the air mass fraction is

$$f_{\mathrm{gH}} = \begin{cases} f_{\mathrm{g0}}, p \le p_{\mathrm{v}}, \\ f_{\mathrm{g0}}\left(1 - 10k_{\mathrm{g}}^3 + 15k_{\mathrm{g}}^4 - 6k_{\mathrm{g}}^5\right), p_{\mathrm{v}} < p \le p_{\mathrm{s}}, \\ 0, p > p_{\mathrm{s}}, \end{cases} \tag{16}$$

where p_{v} is the saturated vapor pressure (Pa), p_{s} is the air apart pressure (Pa), and k_{g} is expressed as

$$k_{\mathrm{g}} = \frac{p - p_{\mathrm{v}}}{p_{\mathrm{s}} - p_{\mathrm{v}}}, \tag{17}$$

2. f_{g} is the instantaneous air mass fraction. When f_{g} is lower than f_{gH}, air should be released from the liquid; otherwise, it should dissolve gradually.

When $f_{\mathrm{g}} \le f_{\mathrm{gH}}$, the air release equation is

$$\frac{\mathrm{d}f_{\mathrm{g}}}{\mathrm{d}t} = a_{21}\sqrt{k}\frac{\rho_{\mathrm{l}}\rho_{\mathrm{l}}}{\rho}\left[\left|P'' - \frac{4}{9}a_{21}\sigma\sqrt{k}\right|\right]^{1/2}\left(f_{\mathrm{gH}} - f_{\mathrm{g}}\right), \tag{18}$$

where a_{21} is coefficient of air release.

Meanwhile, P'' can be written as

$$P'' = \frac{2}{3}\left(\frac{p_{\mathrm{s}} - p}{\rho_{\mathrm{l}}}\right). \tag{19}$$

When $f_{\mathrm{g}} > f_{\mathrm{gH}}$, the dissolution of air is expressed as

$$\frac{\mathrm{d}f_{\mathrm{g}}}{\mathrm{d}t} = -a_{22}\sqrt{k}\frac{\rho_{\mathrm{l}}\rho_{\mathrm{l}}}{\rho}\left[\left|P'' - \frac{4}{9}a_{22}\sigma\sqrt{k}\right|\right]^{1/2}f_{\mathrm{g}}, \tag{20}$$

where a_{22} is the coefficient of air dissolution.

2.2 Dynamic Mass Fraction of Air Components

As the pressure of the aerated hydraulic fluid changes, the density of each component changes accordingly. Based on the air state equation, the air density is written as

$$\rho_{\mathrm{g}} = \rho_{\mathrm{g0}}\left(\frac{p}{p_0}\right)^{1/\lambda}, \tag{21}$$

where p_0 is the standard atmospheric pressure (Pa), ρ_{g0} the air density under the standard atmospheric pressure (kg/m^3), and λ the variability index of the air variable course.

The vapor density is expressed as

$$\rho_{\mathrm{v}} = \rho_{\mathrm{v0}}\left(\frac{p}{p_{\mathrm{v}}}\right)^{1/\lambda}, \tag{22}$$

where ρ_{v0} is the density of vapor under the standard atmospheric pressure (kg/m^3).

Eqs. (21) and (22), show that the air-phase density in the aerated hydraulic fluid is directly related to the variability index in the air variable course. The course of air expansion and compression is typically regarded as either isothermal or adiabatic, which implies that the variability index is a constant. However, the course of air expansion and compression is typically not completely isothermal or adiabatic in actual circumstances; thus, the variability index must be adjusted based on the operating conditions. The volumetric change rate ε, which reflects the rate of air volume change, is the main factor affecting the air variability index. A functional relationship is assumed to exist between ε and λ, i.e., $\lambda = f(\varepsilon)$. Based on the theory of the air variable course, the function must satisfy the following conditions:

(1) When the volumetric changing rate approaches zero, the air variable course becomes isothermal, i.e., $\lim_{\varepsilon\to 0} f(\varepsilon) = \lambda_{\mathrm{iso}}$.
(2) When the volumetric changing rate approaches infinity, the air variable course becomes adiabatic, i.e., $\lim_{\varepsilon\to\infty} f(\varepsilon) = \lambda_{\mathrm{adi}}$.
(3) When ε varies from zero to infinity continuously and monotonously, its first and second derivatives exist, and they are continuous with unchanged signs.

By constructing a function that satisfies the conditions mentioned above, λ can be expressed as follows:

$$\lambda = \frac{\lambda_{\text{iso}}}{1+\mathrm{e}^{\varepsilon/M}} + \frac{C_{\text{n}}/C_{\text{v}} - \lambda_{\text{adi}}}{2C_{\text{n}}/C_{\text{v}} - 1} + 2\sqrt{\frac{C_{\text{n}}}{C_{\text{v}}}\ln\left(\frac{T}{T_0}\right)}, \tag{23}$$

where λ_{iso} is a multivariable index of the isothermal course, M a multivariable course coefficient, C_{n} the molar heat capacity of air (J/mol·K), C_{v} the molar heat capacity of air (J/mol·K), λ_{adi} a multivariable index of the adiabatic course, and T_0 the initial temperature (K).

The molar heat capacity of air can be expressed as [31]

$$C_{\text{n}} = \frac{S_m - S_{m0}}{\ln(T/T_0)}, \tag{24}$$

where S_m is the entropy of air(J/mol·K), and S_{m0} is the entropy of air at the initial temperature (J/mol·K).

The density of the liquid can be expressed as

$$\rho_l = \rho_{\text{l}0} e^{\frac{p-p_0}{E_{\text{l}}}}, \tag{25}$$

where $\rho_{\text{l}0}$ is the density of the liquid at the standard atmospheric pressure (kg/m^3), and E_{l} is the bulk modulus of the liquid at the transient pressure (Pa).

When the pressure and temperature change, the bulk modulus of the liquid changes accordingly. The relationship among the bulk modulus of the liquid, pressure, and temperature can be expressed as follows:

$$E_{\text{l}} = E_{\text{ref}} + m\Delta p + n\Delta T, \tag{26}$$

where E_{ref} is the bulk modulus of the liquid under the standard atmospheric pressure (Pa), m the pressure changing coefficient of the bulk modulus, and n the temperature changing coefficient of the bulk modulus.

Combining Eqs. (21), (22), and (25), the gross density of the aerated hydraulic fluid is expressed as follows:

$$\frac{1}{\rho} = \frac{f_{\text{v}}}{\rho_{\text{v}}} + \frac{f_{\text{g}}}{\rho_{\text{g}}} + \frac{1-f_{\text{v}}-f_{\text{g}}}{\rho_{\text{l}}}, \tag{27}$$

2.3 Dynamic Mass Fraction of Air Components

The bulk modulus reflects the compression characteristics of the aerated hydraulic fluid and is expressed as follows:

$$E = -V\frac{\partial p}{\partial V}, \tag{28}$$

where V is the total fluid volume (m^3).

An aerated hydraulic fluid typically includes three phases: liquid, vapor, and air. In general, an aerated hydraulic fluid contains fewer air-phase components; therefore, it is generally assumed that volume changes among the abovementioned components do not occur. Thus, Eq. (28) can be written as follows:

$$E = -\frac{V}{\frac{\mathrm{d}V_{\text{l}}}{\mathrm{d}p} + \frac{\mathrm{d}V_{\text{g}}}{\mathrm{d}p} + \frac{\mathrm{d}V_{\text{v}}}{\mathrm{d}p}}. \tag{29}$$

Based on the equation of the changeful course of air, the volumes of air and vapor are expressed as

$$V_{\text{g}} = V_{\text{g}0}\left(\frac{p}{p_0}\right)^{1/\lambda}, \tag{30}$$

$$V_{\text{v}} = V_{\text{v}0}\left(\frac{p}{p_0}\right)^{1/\lambda}, \tag{31}$$

where $V_{\text{g}0}$ and $V_{\text{v}0}$ are the air and vapor volumes (m^3) under the standard atmospheric pressure, respectively.

The relationship between the liquid volume and pressure is [21]

$$V_1 = V_{10} e^{\frac{p-p_0}{E_{\text{l}}}}, \tag{32}$$

By calculating the derivative with respect to the pressure using Eqs. (30)–(32) and substituting the obtained derivatives into Eq. (28), the theoretical model of dynamic bulk modulus of an aerated hydraulic fluid can be expressed as

$$E = \frac{1}{A+B+C}, \tag{33}$$

where

$$A = \frac{\rho f_{\text{g}}(t)}{\rho_{\text{g}}\lambda p}, \tag{34}$$

$$B = \frac{\rho f_{\text{v}}(t)}{\rho_{\text{v}}\lambda p}, \tag{35}$$

and

$$C = \frac{\rho_{\text{g}}\rho_{\text{v}} - \rho\rho_{\text{v}} f_{\text{g}}(t) - \rho\rho_{\text{g}} f_{\text{v}}(t)}{\rho_{\text{g}}\rho_{\text{v}} E_{\text{l}}}. \tag{36}$$

3 Numerical Results and Analysis

The proposed theoretical model of dynamic bulk modulus for an aerated hydraulic fluid (Model 1) was applied to calculate the dynamic bulk modulus of the Shell Tellus S ISO32 standard air-containing oil. Table 1 lists the relevant parameters, and Figure 1 shows the pressure variation law of the aerated hydraulic fluid.

Table 1 Parameters of aerated hydraulic fluid

Parameters	Value
Initial density of aerated hydraulic fluid ρ_0 (kg/m^3)	840
Initial density of air ρ_{g0} (kg/m^3)	1.2
Initial bulk modulus of the aerated hydraulic fluid E_0 (Pa)	1.32×10^{10}
Air apart pressure p_s (Pa)	1.013×10^5
Saturated distillation pressure p (Pa)	3×10^3
Initial mass fraction of aerated hydraulic fluid f_{g0}	8.099×10^{-6}
Standard atmosphere pressure p_0 (Pa)	1.013×10^5
Air dissolution coefficient a_{22}	68
Air release coefficient a_{21}	8000

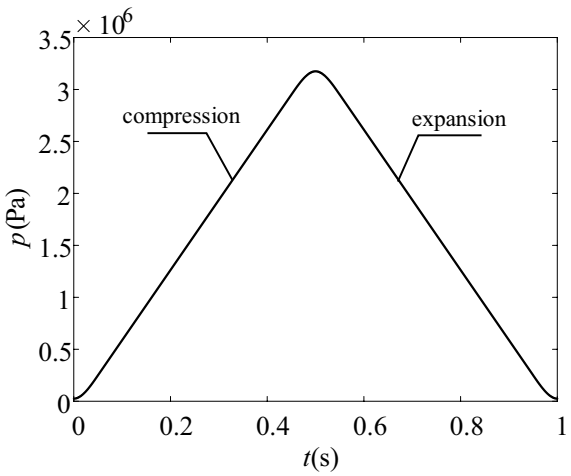

Figure 1 Pressure variation law of aerated hydraulic fluid

From Figure 1, we can see that the pressure of the aerated hydraulic fluid initially increased and then decreased. In other words, the aerated hydraulic fluid is first in the pressurized compression stage and then expanded under reduced pressure, where 3×10^4 Pa is the minimum value of the pressure of the aerated hydraulic fluid, with a maximum value of 3.2×10^6 Pa. The change period for the entire course was 1s. By taking Model 1 as the basic model, Figure 2 shows the numerical results of the dynamic bulk modulus.

Figure 2 shows that during compression, the dynamic bulk modulus of the aerated hydraulic fluid increases with the pressure, whereas during expansion, it decreases with the pressure and finally reached the original value. Although the pressure of the aerated hydraulic fluid remains below the air apart pressure at the initial time of compression, the dynamic air fraction of the aerated hydraulic fluid at that instant remains larger than the calculated value under the initial pressure. Meanwhile, the free air gradually dissolves, which causes the pressure of

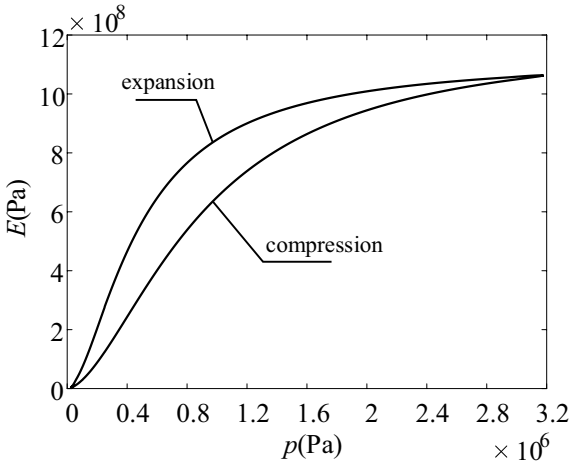

Figure 2 Pressure variation law of the aerated hydraulic fluid

the aerated hydraulic fluid to continue to increase, resulting in an increase in the density of both the air and aerated hydraulic fluid. Thus, the dynamic bulk modulus of the aerated hydraulic fluid increases when the pressure increases from an initial value of 3×10^3 Pa to the air apart pressure of 1.013×10^5 Pa. When the pressure remains above the air apart pressure, the air in the aerated hydraulic fluid continues to dissolve as the pressure increases, thereby resulting in an increase in its dynamic bulk modulus. During expansion, when the ambient pressure remains above the air apart pressure, even though the pressure of the aerated hydraulic fluid is reduced, the air in the oil continues to dissolve as the pressure remains higher than the air apart pressure, and the dynamic air fraction of the aerated hydraulic fluid remains larger than the calculated value. During the course, the air fraction of the aerated hydraulic fluid continues to decrease, resulting in an increase in its bulk modulus; however, the pressure of the oil continues to increase, causing the densities of the air and oil to decrease continuously, and hence a decreasing bulk modulus. Furthermore, the bulk modulus of the aerated hydraulic fluid decreases with the pressure. When the pressure decreases below the air apart pressure and the dynamic air fraction of the aerated hydraulic fluid is smaller than the calculated value, air begins to be released from the oil. Moreover, because the release rate of air during expansion is higher than that during dissolution, a significant amount of air is ejected from the oil in a short period, causing its bulk modulus to continue to decrease and eventually return to its original value at the beginning of the calculation. The dynamic bulk modulus of the aerated hydraulic fluid shows hysteresis during compression and expansion. In other words, under identical instant pressures, the dynamic bulk modulus during

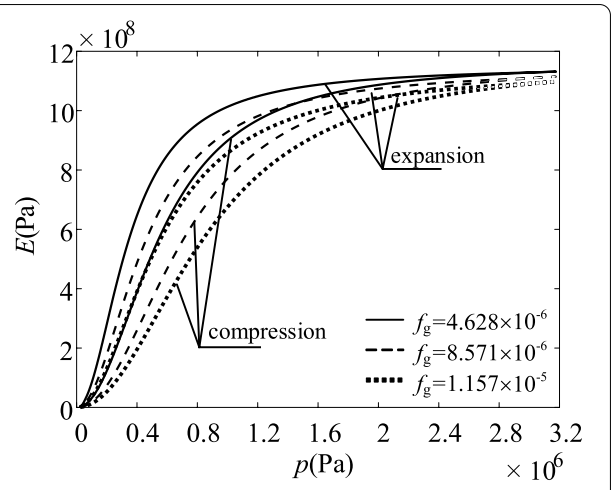

Figure 3 Variation curve of dynamic bulk modulus for different initial air fractions

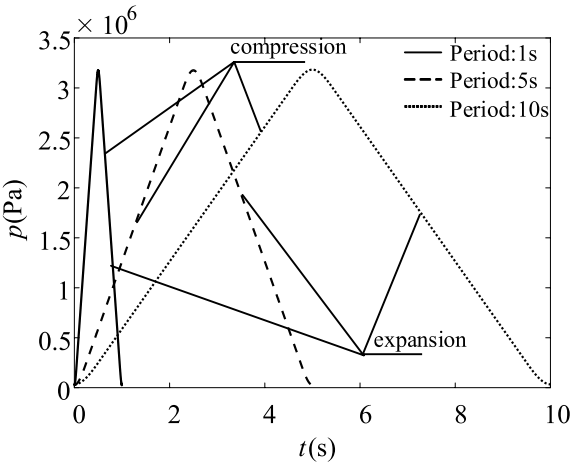

Figure 4 Variation curve of pressure for different pressure changing periods

expansion is larger than that during compression. This is because the proportion of free air in the mixed fluid during compression is greater than that during expansion.

4 Analysis of Influencing Factors

4.1 Analysis of Influencing Factors Based on Different Initial Air Fractions

Based on the pressure shown in Figure 1 and by considering the aerated hydraulic fluid parameters shown in Table 1, the effect of air fraction on the dynamic bulk modulus is shown in Figure 3.

As shown in Figure 3, at identical pressures, the higher the initial rate of the containing air, the smaller is the dynamic bulk modulus. This is attributable to the pressure, which significantly affects the rate of release and dissolution of air. Under a certain pressure, the air release and dissolution rates are defined as well. The amount of remaining free air increases with the initial rate of containing air under identical pressures, whereas the bulk modulus of the aerated hydraulic fluid decreases.

4.2 Analysis of Influencing Factors Based on Different Pressure Changing Periods

Based on the pressure variation law of the aerated hydraulic fluid shown in Figure 1, the periods of air expansion and compression changed, and the pressure variation law of the aerated hydraulic fluid under different periods is obtained, as shown in Figure 4.

Subsequently, using the parameters of the aerated hydraulic fluid shown in Table 1, the result shows that the mean flow rate changes based on the pressure-changing period. Because the coefficients of air dissolution and release are related to the fluid velocity, the coefficients change accordingly. Table 2 shows the coefficients of the air release and dissolution based on pressure changing periods of 1, 5, and 10 s. The variation curve of dynamic bulk modulus at different pressure-changing cycles under identical initial rates of containing air is shown in Figure 5.

Table 2 Coefficients of air release and dissolution for different pressure changing periods

Pressure variation period (s)	Air dissolution coefficient	Air release coefficient
1	68	8000
5	350	40000
10	5000	80000

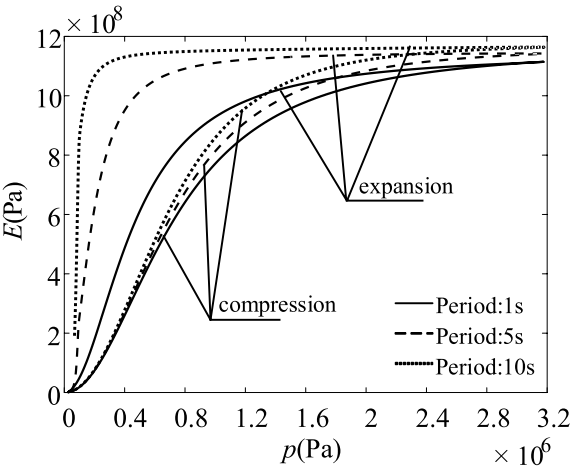

Figure 5 Variation curve of dynamic bulk modulus for different pressure changing periods

As shown in Figure 5, under identical air fractions, the longer the pressure-changing period, the larger is the bulk modulus of the aerated hydraulic fluid. This is because under identical air fractions, the longer the pressure changing period, the longer the aerated hydraulic fluid remains above the air apart pressure, which implies a larger amount of dissolved air and less free air. When the pressure changing period is 10 s, the bulk modulus during compression reaches 1.16×10^9 Pa when the pressure reaches 2.975×10^6 Pa and remains invariant thereafter. While the aerated hydraulic fluid expands under reduced pressure, during the period when the pressure decreases from 3.2×10^6 Pa to 1.013×10^5 Pa (air apart pressure), the dynamic bulk modulus remains invariant at 1.16×10^9 Pa until the pressure decreases below the air apart pressure. Subsequently, the dynamic bulk modulus decreases rapidly to its original value. This is because under the pressure change period of 10 s, the pressure changing period of the aerated hydraulic fluid is sufficiently long to allow the pressure to remain above the air apart pressure. During compression, when the pressure reaches 2.975×10^6 Pa, most of the air in the aerated hydraulic fluid has dissolved. Simultaneously, the bulk modulus of the liquid increases slightly with the pressure; therefore, even when the pressure continues to increase, the dynamic bulk modulus does not change significantly, i.e., it increases only slightly by 1.16×10^9 Pa. Meanwhile, because the air contained in the hydraulic oil dissolved during compression, air will not be released from the oil during expansion provided that the pressure remains above the air apart pressure. Thus, the oil remains in the liquid state, and the bulk modulus of the liquid phase decreases with pressure. When the pressure decreases from 3.2×10^6 to 1.013×10^5 Pa, the dynamic bulk modulus increases only slightly and remains invariant at 1.16×10^9 Pa; when the pressure is lower than the air apart pressure, air be ejected from the fluid immediately, and the dynamic bulk modulus will increase rapidly.

4.3 Analysis of Influencing Factors Based on Different Temperatures

Using the parameters of the aerated hydraulic fluid listed in Table 1, the variation curve of dynamic bulk modulus at different temperatures under the pressure shown in Figure 1 is shown in Figure 6.

Figure 6 shows that whereas the initial air fraction and pressure changing period are the same, the dynamic bulk modulus decreases with temperature at the same pressure point. This is because, when the temperature increases, the volume of the aerated hydraulic fluid expands, resulting in a decrease in the densities of the oil and bulk modulus. In addition, as the temperature increases, the thermal motion of the air molecules accelerates, air tends

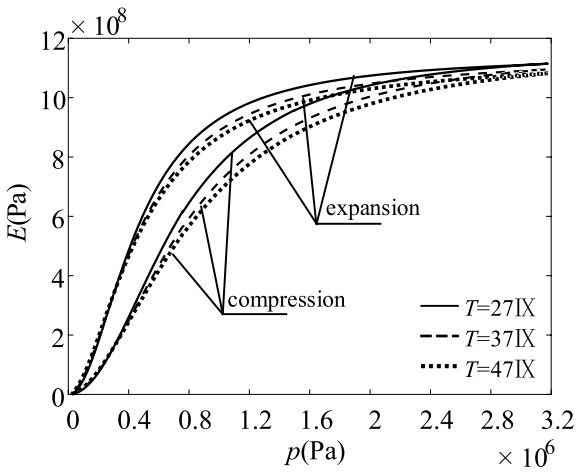

Figure 6 Variation curve of dynamic bulk modulus for different temperatures

to be released from the aerated hydraulic fluid, and the proportion of free air in the mixed fluid increases, which results in a decrease in the bulk modulus. The trend of the bulk modulus with temperature varies under different pressures. When the pressure is less than 4×10^5 Pa, the bulk modulus changes slightly with temperature. This is due to the high air fraction of the aerated hydraulic fluid in the low-pressure stage. The change in the air state caused by temperature change does not significantly affect the bulk modulus, thereby resulting in the low sensitivity of the bulk modulus to temperature. Therefore, at this stage, the bulk moduli at different temperatures are similar. When the pressure exceeds 4×10^5 Pa, the variation in the bulk modulus with temperature is significant. This is because, as the pressure increases, the air fraction continues to decrease, resulting in a change in the air state change caused by the significant effect of the temperature change on the bulk modulus. In other words, the bulk modulus is sensitive to temperature; thus, the bulk modulus varies significantly at different temperatures.

5 Model Validation

5.1 Experimental Verification

While investigating the effective bulk modulus of hydraulic oil, Bin [28] measured the bulk modulus of L-HM46 anti-wear hydraulic oil containing a certain amount of air during compression. The experimental setup is shown in Figure 7. The test bench primarily includes the following three components: A closed hydraulic power system with controllable air content, bulk modulus detection device, and hydraulic servo cylinder system. The closed hydraulic system can isolate the oil from the atmosphere, thereby significantly reducing the effect of the external atmospheric environment on the parameters of the hydraulic system.

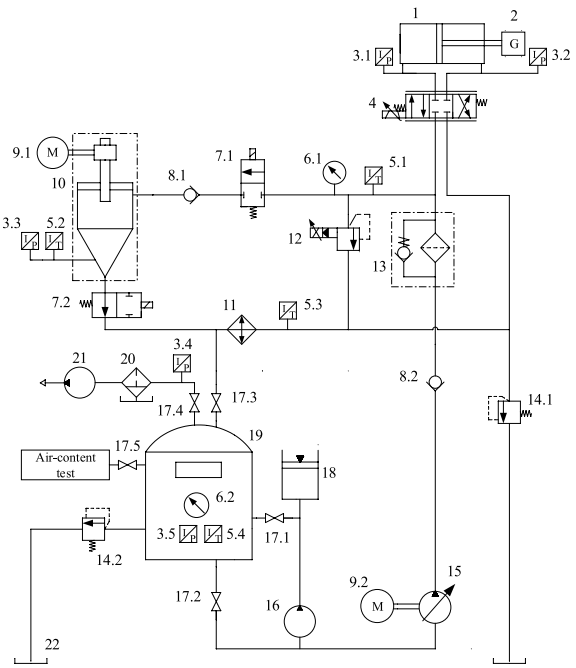

Figure 7 Schematic diagram of experimental system for measuring bulk modulus: 1. Servo cylinder, 2. Heavy block, 3. Pressure sensor, 4. Servo valve, 5. Temperature sensor, 6. Pressure gauge, 7. Electromagnetic directional valve, 8 Check valve, 9. Motor, 10. Elastic modulus measuring device body, 11. Air cooler, 12. Proportional relief valve, 13. Main oil line filter, 14. Overflow valve, 15. Constant pressure variable pump, 16. Manual suction pump, 17. Ball valve, 18. Auxiliary oil tank, 19. Stirring oil tank, 20. Oil-water filter, 21. Vacuum pump, 22. Main oil tank

The bulk modulus detection device obtains the pressure and volume of the oil in the test cavity through hydraulic loading and then calculates the value of the bulk modulus using Eq. (28). A hydraulic servo cylinder system is used as a supplementary system for the detection device. The research method is to fix the other parameters but compare and analyze the difference in system performance by changing the bulk modulus of the oil. The effect of the dynamic change in the bulk modulus was verified based on the change in the system characteristics.

The authors of Ref. [17] measured the bulk modulus of an aerated hydraulic fluid during compression at different temperatures. By applying the experimental results presented in the abovementioned reference as a basis, comparing the theoretical value of Model 1 during the compression course with the experimental data, and using the goodness-of-fit calculated using the theoretical model as the evaluation index, the effectiveness and accuracy of the dynamic bulk modulus can be expressed as follows:

$$R^2 = 1 - \frac{\sum \left(y_i - \widehat{y_i}\right)^2}{\sum \left(y_i - \overline{y_i}\right)^2}, \tag{37}$$

where y_i is the theoretical calculation result of the dynamic bulk modulus at the ith point, $\widehat{y_i}$ the experimental measurement result at the ith point, and $\overline{y_i}$ the mean value of the theoretically computed results.

The parameters used in Ref. [17] for the aerated hydraulic fluid are listed in Table 3, and Figure 8 shows a comparison between the calculated values and experimental data.

Theoretically, under the same pressure, the bulk modulus decreases with increasing temperature. As shown in Figure 8, when the pressure exceeds 2×10^6 Pa, the experimental value of the bulk modulus at the same pressure point decreases as the temperature increases. When the pressure is within 2×10^6 Pa, the experimental values at each temperature point under the same pressure point are relatively similar; however, beyond

Table 3 Parameters pertaining to aerated hydraulic fluid

Parameters	Value
Initial density of the aerated hydraulic fluid (kg/m^3)	850
Initial density of air (kg/m^3)	1.29
Initial bulk modulus of the hydraulic oil (Pa)	1.8×10^9
Air apart pressure (Pa)	2.4×10^6
Initial mass fraction of the aerated hydraulic fluid	1.95×10^{-6}
Standard atmosphere pressure (Pa)	1.013×10^5
Air dissolution coefficient	30
Air release coefficient	4000

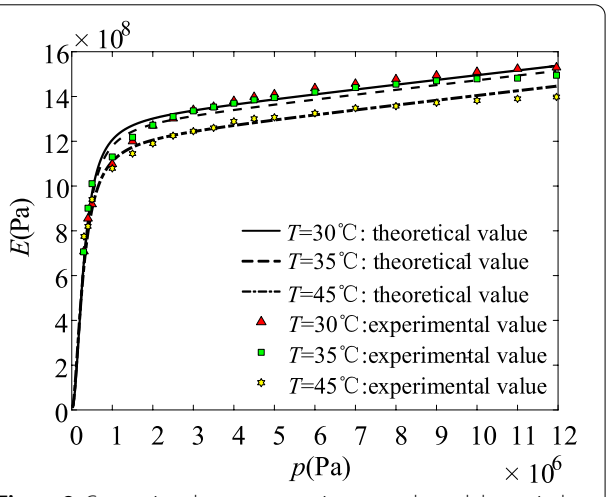

Figure 8 Comparison between experiment results and theoretical dynamic model of dynamic bulk modulus

the abovementioned pressure, the value fluctuates significantly. This phenomenon is attributable to the following reasons: Because the air fraction of the fluid is high at lower pressures, the temperature does not significantly affect the bulk modulus; subsequently, as the pressure increases, the air continues to dissolve, the air fraction of the fluid decreases, and the bulk modulus of the oil becomes increasingly sensitive to the temperature. During compression, when the oil temperature is 30 °C, the goodness-of-fit between the theoretical value of the dynamic bulk modulus calculated using Model 1 and the experimental value is 0.9726. Meanwhile, at oil temperatures of 35 °C and 45 °C, the goodness-of-fit is 0.9732 and 0.9675, respectively. Therefore, Model 1 can accurately predict the dynamic performance of an aerated hydraulic fluid following pressure changes under different temperature conditions.

6 Conclusions

(1) For an aerated hydraulic fluid, based on the full cavitation model and improved Henry's law, the transient air fraction of air components in the fluid under the effects of pressure and temperature was derived by applying the lumped parameter method. Using the multivariable exponential model, the transient density of each component in the fluid was derived while the temperature was changed by introducing thermodynamic parameters. A theoretical model of the dynamic bulk modulus of an aerated hydraulic fluid was established by determining the transient air fraction and transient density of the aerated hydraulic fluid.

(2) Using Model 1 to calculate the dynamic bulk modulus of the Shell Tellus S ISO 32 standard air-containing oil, the results showed that the dynamic bulk modulus of the aerated hydraulic fluid during expansion and compression was inconsistent owing to the different fractions of free air during the two abovementioned courses. Furthermore, at identical pressure points, the dynamic bulk modulus of the compression course was lower than that of the expansion course.

(3) The effects of the initial air fraction, period of pressure change, and temperature on the dynamic bulk modulus were analyzed. Under the same pressure-changing cycle and temperature, the dynamic bulk modulus decreased as the initial air fraction increased. Under the same initial air fraction and temperature, the longer the pressure-changing cycle, the greater was the dynamic bulk modulus at identical pressure points. When both the initial air fraction and pressure-changing cycle were the same, the dynamic bulk modulus was lower at higher temperatures. The dynamic bulk modulus at each temperature point was similar at low pressures.

(4) By comparing Model 1 with the experimental results at different temperatures during compression, the goodness-of-fit between the theoretical model and experimental value was 0.9726, 0.9732, and 0.9675 at 30 °C, 35 °C, and 45 °C, respectively. This shows that the theoretical values fitted well with the experimental values, which implies that the proposed Model 1 can accurately predict the dynamic bulk modulus of the aerated hydraulic fluid under steady-state conditions until a pressure of 1.2×10^7 Pa for different temperatures.

Acknowledgements
Not applicable.

Authors' Contributions
XY and LZ conducted the entire experiment; W W wrote the manuscript; XZ assisted with sampling and laboratory analyses. All authors read and approved the final manuscript.

Authors' Information
Xiaoming Yuan, born in 1984, is currently an associate professor at *Yanshan University, China*. He received his PhD degree from *Yanshan University, Qinhuangdao, China*, in 2014. His research interests include fluid–structure interaction dynamics of firefighting monitors, fluid transmission and control, and new magnetic gear transmission and control.
Weiqi Wang received his B.S. degree from *School of Mechanical Engineering, Yanshan University, China*, in 2020, where he is currently pursuing his Master's degree. His research interests include fluid transmission and control.
Xuan Zhu received his Master's degree from *School of Mechanical Engineering, Yanshan University, China*, in 2020. His research interests include fluid transmission and control, and fluid system simulations.
Lijie Zhang, born in 1969, is currently the vice-president of *Hebei Agricultural University, China*. He received his PhD degree from *Yanshan University, China*, in 2006. His research interests include the reliability and fault diagnosis of hydraulic components, multiphysics coupling analysis, mechanics, and robotics.

Funding
Supported by National Natural Science Foundation of China (Grant Nos. 52175066, 51805468), Hebei Provincial National Natural Science Foundation of China (Grant No. E2020203090), Science and Technology Project of Hebei Education Department of China (Grant No. ZD2022052) and Open Foundation of the Key Laboratory of Fire Emergency Rescue Equipment of China (Grant No. 2020XFZB07).

Competing Interests
The authors declare no competing financial interests.

Author Details
[1]Hebei Key Laboratory of Heavy Machinery Fluid Power Transmission and Control, Yanshan University, Qinhuangdao 066004, China. [2]Key Laboratory of Advanced Forging & Stamping Technology and Science, Ministry of Education of China, Yanshan University, Qinhuangdao 066000, China. [3]State Key Laboratory of Fluid Power and Mechatronic Systems, Zhejiang University, Hangzhou 310027, China.

Received: 7 July 2021 Revised: 2 April 2022 Accepted: 22 April 2022
Published online: 23 September 2022

References

[1] Y Zhu, S N Tang, C Wang, et al. Bifurcation characteristic research on the load vertical vibration of a hydraulic automatic gauge control system. *Processes*, 2019, 7(10).

[2] Y Zhu, P F Qian, S N Tang, et al. Amplitude-frequency characteristics analysis for vertical vibration of hydraulic AGC system under nonlinear action. *AIP Advances*, 2019, 9(3).

[3] L T Lyu, Z Chen, B Yao. Energy saving motion control of independent metering valves and pump combined hydraulic system. *IEEE/ASME Transactions on Mechatronics*, 2019, 24(5):1909–1920.

[4] P Qian, C Pu, L Liu, et al. Development of a new high-precision friction test platform and experimental study of friction characteristics for pneumatic cylinders. *Measurement Science and Technology*, 2022, 33(6): 065001

[5] Y Zhu, S N Tang, C Wang, et al. Absolute stability condition derivation for position closed-loop system in hydraulic automatic gauge control. *Processes*, 2019, 7(10).

[6] Q Gao. Nonlinear adaptive control with asymmetric pressure difference compensation of a hydraulic pressure servo system using two high speed on/off valves. *Machines*, 2022, 10(1): 66.

[7] J Y Yao, W X Deng. Active disturbance rejection adaptive control of hydraulic servo systems. *IEEE Transactions on Industrial Electronics*, 2019, 66(10): 8023–8032.

[8] Z K Yao, J Y Yao, W C Sun. Adaptive rise control of hydraulic systems with multilayer neural-networks. *IEEE Transactions on Industrial Electronics*, 2019, 66(11): 8638–8647.

[9] L T Lyu, Z Chen, B Yao. Development of pump and valves combined hydraulic system for both high tracking precision and high energy efficiency. *IEEE Transactions on Industrial Electronics*, 2019, 66(9): 7189–7198.

[10] Q Gao, Y Zhu, J H Liu. Dynamics modelling and control of a novel fuel metering valve actuated by two binary-coded digital valve arrays. *Machines*, 2022, 10(1): 55.

[11] X M Yuan, X Zhu, C Wang, et al. Research on theoretical model of dynamic bulk modulus of air-containing hydraulic oil. *IEEE ACCESS*, 2019, 7: 178413–178422.

[12] J H Seung, S G Yoo, N O Seul, et al. Unknown-parameter estimation of electric-hydraulic servo cylinder based on measurements. *IEMEK Journal of Embedded Systems and Applications*, 2019, 14(6): 1–7.

[13] L Hruzik, M VaSina, A Burecek A. Evaluation of bulk modulus of oil system with hydraulic line. *EDP Sciences*, 2013, 45: 01041.

[14] T Bhakta, P Avseth, M Landr. Sensitivity analysis of effective fluid and rock bulk modulus due to changes in pore pressure, temperature and saturation. *Journal of Applied Geophysics*, 2016, 135: 77–89.

[15] G Kim, K W Wang. On-line monitoring of fluid effective bulk modulus using piezoelectric transducer impedance. *Asme International Mechanical Engineering Congress & Exposition*. 2007: 129–136.

[16] Q P Chen, M M Wu, S Kang, et al. Study on cavitation phenomenon of twin-tube hydraulic shock absorber based on CFD. *Engineering Applications of Computational Fluid Mechanics*, 2019, 13(1): 1049–1062.

[17] H Okabe, Y Tanaka, A Watanabe, et al. Cavitation in a spool valve for water hydraulics. *IOP Conference Series: Earth and Environmental Science*, 2019.

[18] J Nykanen. Comparison of different fluid models. *Bath Workshop on Power Transmission and Motion Control*. University of Bath, 2000.

[19] P Righettini, R Strada, S Valilou, et al. Nonlinear model of a servo-hydraulic shaking table with dynamic model of effective bulk modulus. *Mechanical Systems and Signal Processing*, 2018, 110: 248–259.

[20] T Kato, Y Xu, T Tanaka, et al. Force control for ultraprecision hybrid electric-pneumatic vertical-positioning device. *International Journal of Hydromechatronics*, 2021, 4(2): 185–201.

[21] A M Hurst, J VanDeWeert. A study of bulk modulus, entrained air, and dynamic pressure measurements in liquids. *Journal of Engineering for Gas Turbines and Power*, 2016, 138(10): 101601–101601

[22] A K Singhal, M M Athavale, H Y Li, et al. Mathematical basis and validation of the full cavitation model. *Journal of Fluids Engineering*, 2002, 124(3): 617–624.

[23] J Zhou, A Vacca, B Manhartsgruber. A novel approach for the prediction of dynamic features of air release and absorption in hydraulic oils. *Journal of Fluids Engineering*, 2013, 135(9): 1–8.

[24] S Sakama, Y Tanaka, H Goto. Mathematical model for bulk modulus of hydraulic oil containing air bubbles. *Mechanical Engineering Journal*, 2015, 2(6): 1–10.

[25] A Sojoudi, A Nourbakhsh, H Shokouhmand. Establishing a relationship between hydraulic efficiency and temperature rise in centrifugal pumps: experimental study. *Journal of Hydraulic Engineering*, 2018, 144(4). https://doi.org/10.1061/(ASCE)HY.1943-7900.0001442

[26] W Han, L Xiong, Z P Yu. A novel pressure control strategy of an electro-hydraulic brake system via fusion of control signals. *Proceedings of the Institution of Mechanical Engineers Part D Journal of Automobile Engineering*, 2019, 233(13): 3342–3357.

[27] S Kim, U H Murrenhoff. Measurement of effective bulk modulus for hydraulic oil at low pressure. *Journal of Fluids Engineering*, 2012, 134(2): 1–10.

[28] F Bin. *Research on bulk modulus of hydraulic oil and measuring device*. Zhejiang: Zhejiang University, 2011. (in Chinese)

[29] H L Yi, J X Tian. Corresponding states correlation for temperature dependent surface tension of normal saturated liquids. *International Journal of Modern Physics B*, 2014, 28(25).

[30] S N Shreya, V Rodriguez-Martinez, M O'Meara, et al. Density, viscosity, and surface tension of five vegetable oils at elevated temperatures: Measurement and modeling. *International Journal of Food Properties*, 2017, 20(S2): S1965–S1981.

[31] E W Lemmon, R T Jacobsen, S G Penoncello, et, al. Thermodynamic properties of air and mixtures of nitrogen, argon, and oxygen from 60 to 2000 K at pressures to 2000 MPa. *Journal of Physical & Chemical Reference Data*, 2000, 29(3).